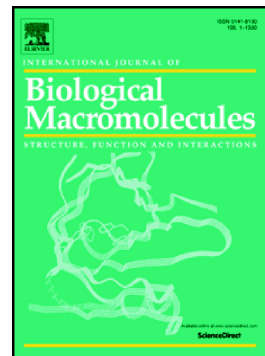# Journal Pre-proof

Bio-derived Schiff base vitrimer with outstanding flame retardancy, toughness, antibacterial, dielectric and recycling properties

Guofeng Ye, Cheng Wang, Qi Zhang, Pingan Song, Hao Wang, Siqi Huo, Zhitian Liu

Please cite this article as: G. Ye, C. Wang, Q. Zhang, et al., Bio-derived Schiff base vitrimer with outstanding flame retardancy, toughness, antibacterial, dielectric and recycling properties, *International Journal of Biological Macromolecules* (2024), https://doi.org/10.1016/j.ijbiomac.2024.134933

Bio-derived Schiff base vitrimer with outstanding flame retardancy, toughness, antibacterial, dielectric and recycling properties

Guofeng Ye[a], Cheng Wang[a], Qi Zhang[a,*], Pingan Song[c], Hao Wang[b], Siqi Huo[b,*], Zhitian Liu[a,*]

[a] *Hubei Engineering Technology Research Centre of Optoelectronic and New Energy Materials, School of Materials Science & Engineering, Wuhan Institute of Technology, Wuhan 430205, China*

[b] *School of Engineering, Centre for Future Materials, University of Southern Queensland, Springfield 4300, Australia*

[c] *School of Agriculture and Environmental Science, Centre for Future Materials, University of Southern Queensland, Springfield 4300, Australia*

[*] Corresponding authors:

E-mail: whzq_2014@163.com (Q. Zhang)

E-mail: sqhuo@hotmail.com and Siqi.Huo@unisq.edu.au (S. Huo)

E-mail: able.ztliu@wit.edu.cn (Z. Liu)

ABSTRACT: Thermosetting resins are widely used in high-tech applications for excellent mechanical robustness and chemical resistance. With increasing attention to the environmental and usage safety issues, it is necessary to develop bio-derived, recyclable, tough, and fire-retardant thermosetting resins. Herein, a high-performance, vanillin-based vitrimer ($CIP_{1.0}$) was prepared. The $CIP_{1.0}$ with 1.0 wt% phosphorus passes vertical burning (UL-94) V-0 rating with a limiting oxygen index (LOI) of 27.2%. The phosphorus-containing and Schiff base groups act synergistically in gas and condensed phases during combustion, endowing $CIP_{1.0}$ with outstanding fire retardancy. The $CIP_{1.0}$ shows excellent toughness with high elongation at break of 45.0% due to the π-π stacking of numerous rigid aromatic groups

1

and appropriate cross-linking density. The highly symmetrical structure and low polarizability of $CIP_{1.0}$ result in a low dielectric constant. The $CIP_{1.0}$ exhibits superior antimicrobial properties. The $CIP_{1.0}$ can be reprocessed by hot-pressing at 140 °C for 10 minutes. The non-destructive, closed-loop recycling of carbon fibers in the carbon fiber-reinforced $CIP_{1.0}$ composite can be achieved under mild conditions due to the degradable Schiff base groups of $CIP_{1.0}$. In this work, a bio-derived, tough, fire-retardant, low dielectric, and antimicrobial vitrimer is prepared to provide a rational strategy for the design of advanced environmentally friendly thermosetting resins.

1. Introduction

Thermosetting resins, as one of the most prominent polymers, are widely adopted as resin matrices or adhesives for fiber-reinforced polymer composites in the automotive, aerospace, electrical equipment, and construction industries due to their outstanding mechanical strength, durability, and electrical insulation [1, 2]. Nevertheless, owing to the stable covalently cross-linked networks, most end-of-life thermosetting resins tend to be burned or buried, which is not in line with the trend towards Carbon Peaking and Carbon Neutrality [3].

Previous works have shown that introducing dynamic covalent bonds (DCBs), *e.g.,* esters, imines, siloxanes, and disulfides, into the crosslinked network can reduce the damage to environment [4-7]. Under external stimuli, *e.g.,* light, heat, and chemicals, the polymers with DCBs undergo bond exchange reactions to achieve topological rearrangements and allow them to be reused. Those thermosetting resins with associative exchange mechanisms are known as vitrimers, and great efforts have recently been devoted to its development. Li *et al.* have prepared transesterification vitrimer using tung oil and maleic anhydride with zinc acetylacetonate as a catalyst [8]. The resulting vitrimer obtained high tensile strength (59.2

2

MPa) and glass transition temperature (76.7 °C) and its scratch recovery rate was 96.7% at 180 °C for 1 hour. However, the catalysts within the vitrimer network may gradually leach out during long-term use, adversely impacting both vitrimer properties and the environment. Therefore, it is imperative to develop catalyst-free vitrimers.

In addition, polymers have high proportions of C, H, and O elements in their structures, which makes them flammable [9]. Enhancing the flame retardancy of vitrimer can further enable its high-tech applications. Chen *et al.* incorporated a phosphaphenanthrene-derived diol (6-(2,5-bis(2-hydroxyethoxy)phenyl)dibenzo[*c*,*e*] [1,2]oxaphosphinine 6-oxide, DHH) into an epoxy/anhydride system, and the obtained vitrimer can be recovered without a catalyst [7]. Meanwhile, due to the presence of the phosphaphenanthrene moiety, the resulting vitrimer easily passed a UL-94 V-0 rating and had an LOI as high as 36.0%. The hydroxy groups served as a catalytic site towards the transesterification reaction, and thus the vitrimer could be remodeled after hot-pressing at 220 °C under 10 MPa for 2 hours. However, the reported flame-retardant vitrimers usually required strict recovery conditions, *e.g.,* high temperatures and pressures [7, 8].

One of the most promising DCBs is the Schiff base, which can be formed by condensation of amines and aldehydes or ketones and hydrolyzed (in acidic conditions) to aldehydes (or ketones) and amines. No catalyst is required for these processes [10-12]. In addition, the activation energy required for Schiff base exchange is much lower than that of transesterification, and it is expected to realize energy-efficient recycling [13]. The Schiff base is considered to have a flame-retardant function, which can undergo carbonization and release non-flammable gases during combustion. Moreover, it has an antibacterial effect. All these effects distinguish Schiff base vitrimers from other kinds of vitrimers [14]. Nevertheless, the previous works on Schiff base vitrimers had been mainly focused on degradation, mechanical properties, and flame retardancy, while the dielectric properties are

less studied. The dielectric properties of polymeric materials are also very important in the fields of electronic devices and high-voltage transformers. Triazine rings have been demonstrated to be favorable for achieving low dielectric constants due to their low polarizability and highly symmetric structure [15, 16]. In this work, we developed a transparent Schiff-based vitrimer with excellent mechanical, flame retardant, dielectric, and antibacterial properties from triazine-containing cyanuric chloride (CC), phenylphosphonic dichloride (PPDC), isophorone diamine (IPDA) and bio-based vanillin. The π-π stacking of numerous aromatic groups within the cross-linked network results in high toughness of the resulting vitrimer, and the highly symmetrical structure also brings about a low dielectric constant. Meanwhile, the presence of phosphate ester and C=N enhances the flame retardancy of the vitrimer. Most importantly, the non-destructive recovery of carbon fibers (CFs) from the carbon fiber reinforced $CIP_{1.0}$ ($CF/CIP_{1.0}$) composites is essentially achieved. Therefore, this work provides a promising approach for the preparation of high-performance, fire-safe Schiff base vitrimers, which are expected to be thermoset alternatives for various applications.

2. Materials and methods

2.1. Materials

Vanillin, CC, PPDC, triethylamine (TEA), IPDA, dichloromethane (DCM), tetrahydrofuran (THF, water ≤ 30 ppm), and *N*, *N*-dimethylformamide (DMF) were purchased from Energy Chemical Co., Ltd. (Shanghai, China). Unidirectional carbon fiber fabric (areal density: 200 g/m^2) was purchased from Zhongfu Shenying Carbon Fiber Co., Ltd. (Jiangsu, China). Escherichia coli (*E*. coli,) and Staphylococcus aureus (*S*. aureus) were provided by People's Hospital of Jiangxi province (Jiangxi, China).

2.2. Synthesis of vanillin-containing CC derivative (CV)

The synthetic route of CV is shown in Fig. 1a. Specifically, vanillin (25.0 g) was added to

a three-necked flask with a condensing unit and nitrogen gas flow. THF (250 mL) was introduced to solubilize vanillin. In addition, TEA (16.7 g) was incorporated into the flask to act as an acid-binding agent. Then, CC (10.0 g) was dissolved in THF (100 mL) and the solution was added dropwise to the flask. The reaction was carried out under magnetic stirring at 0, 30, and 60 °C for 2 hours, respectively. The crude product was obtained by filtration. The final product was collected by washing the crude product sequentially with 25 and 80 °C water. CV (white powder) was obtained by drying in a vacuum oven at 80 °C for 12 hours (Yield: 92.6%).
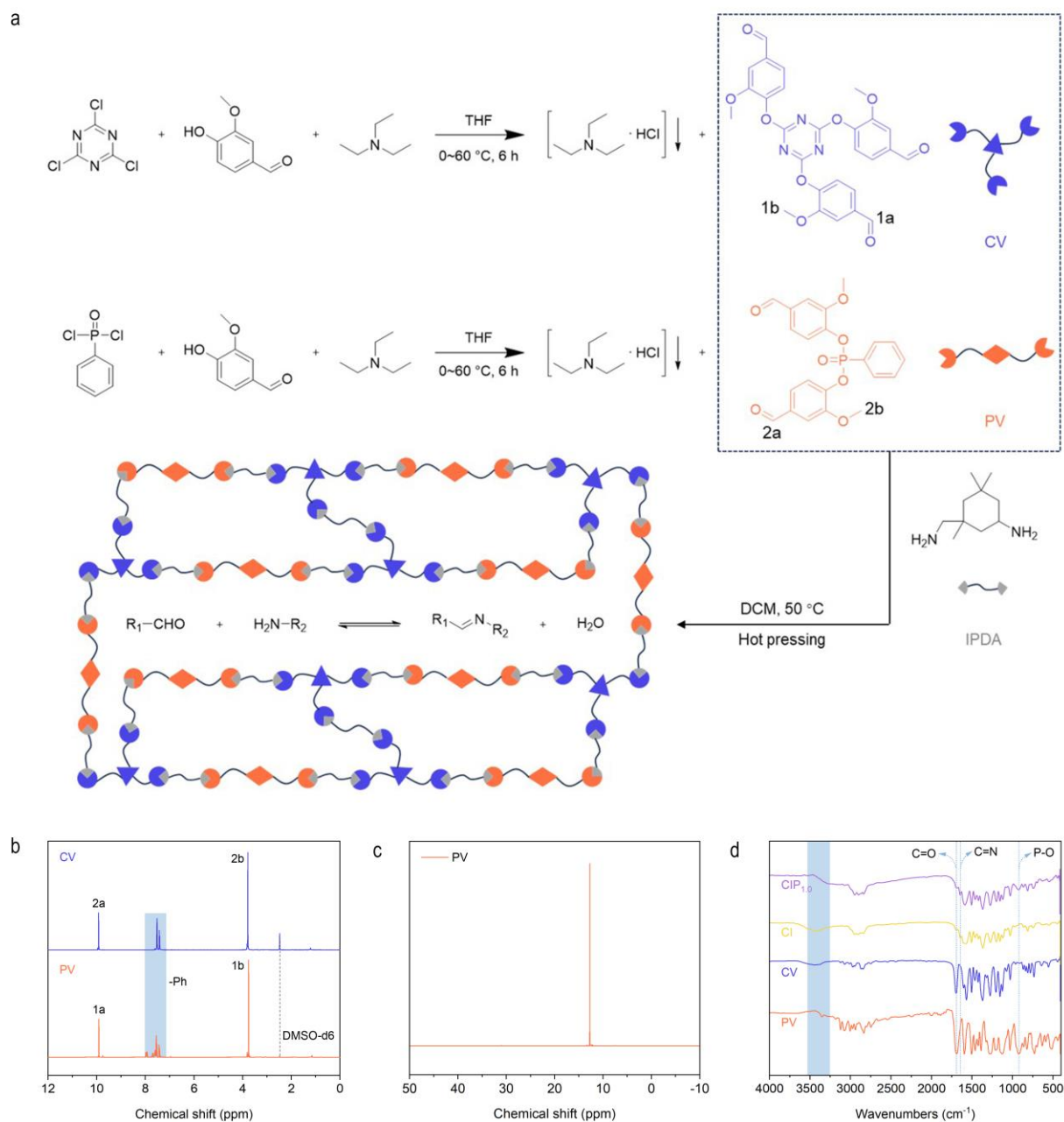
Fig. 1. (a) The synthetic route of CV, PV, and the scheme for the preparation of CIP_x vitrimer; (b) ^1H NMR spectra of CV and PV; (c) ^{31}P NMR spectra of PV; (d) FTIR spectra of CV, PV, CI, and $CIP_{1.0}$.

2.3. Synthesis of vanillin-containing PPDC derivative (PV)

The synthesis of PV is similar to that of CV and its synthesis route is shown in Fig. 1a. Vanillin (15.6 g), THF (156 mL), and TEA (10.4 g) were introduced to a three-necked flask with the condensing unit and nitrogen gas flow. Then, PPDC (10.0 g) was dissolved in THF

(100 mL) and the solution was added dropwise to the flask. The reaction was carried out under magnetic stirring at 0, 30, and 60 °C for 2 hours, respectively. The final PV (yellow solid) was generated by the above purification method (Yield: 86.5%).

2.4. Preparation of vanillin-containing vitrimers and CF/CIP$_{1.0}$

The detailed formulations of vitrimers are shown in Table S1. PV (1.3 g), IPDA (3.1 g), and DCM (10.0 mL) were positioned in a flask with a condensing unit, and they were mixed at 50 °C for 30 minutes. Subsequently, CV (5.3 g) was introduced for cross-linking. After the mixture became gelled, it was placed in a drying oven at 50 °C for 2 hours to remove solvent and then transferred to a vacuum oven at 100 °C for 8 hours to remove water. The resultant CIP$_x$ solids were further cured by hot-pressing at 150 °C for 30 minutes under 10 MPa, and the x was representative of phosphorus content. CI was made with the same method, but no PV was introduced. The CF/CIP$_{1.0}$ composite (the mass ratio of CF : CIP$_{1.0}$ = 6 : 4) was prepared by the combination of hand lay-up and hot-pressing. Before gelling the CIP$_{1.0}$ mixture, it was placed on a glass plate, and then CFs were attached to it. Subsequently, they were placed in a fume hood for 10 minutes, and then the prepreg was obtained. The above steps were repeated six times, and six prepregs were obtained. The prepregs were stacked together and dried in a drying oven at 50 °C for 2 hours and a vacuum oven at 100 °C for 8 hours. Finally, the CF/CIP$_{1.0}$ composite was obtained by hot-pressing at 150 °C for 30 minutes under 10 MPa.

2.5. Characterizations

This section is presented in the Supporting Information.

3. Results and discussion

3.1. Characterization of CV, PV and vitrimer

The chemical structures of CV and PV were characterized *via* nuclear magnetic resonance (NMR) and Fourier transform infrared (FTIR), with the results presented in Fig. 1b-d and S1.

The ^{1}H NMR spectra of CV and PV are shown in Fig. 1b. CV and PV are characterized by similar proton chemical shifts. There are no shifts of phenolic groups in both CV and PV, suggesting that the phenolic group in vanillin is completely reacted by -C-Cl/-P-Cl. The chemical shift at 9.9 ppm is attributed to the aldehyde group in CV and PV, and the chemical shift at 3.8 ppm is attributed to the proton in methyl. The protons of phenyl in both CV and PV appear at 7.2-8.0 ppm. Notably, the integrals of aldehyde : methyl : phenyl in both CV and PV are 1 : 3 : 3. This indicates that CC/PPDC has successfully reacted with vanillin to generate CV and PV. In addition, the ^{13}C NMR spectra of CV and PV are presented in Fig. S1. The chemical shifts of aldehyde and methyl in CV/PV are around 192.0 and 56.5 ppm, respectively. The chemical shift of triazine group in CV can be found at 173.2 ppm. The chemical shifts of phenyl in CV/PV are between 110~152 ppm. There are no additional chemical shifts found in both ^{13}C NMR spectra. Furthermore, PV shows only one peak around 12.5 ppm (see Fig. 1c) in its ^{31}P NMR, which also indicates that it is successfully synthesized and has a high purity.

The FTIR spectra of CV, PV, CI, and CIP$_{1.0}$ are shown in Fig. 1d. Regarding CV and PV, the characteristic absorption peak of -CHO can be detected at 1690 cm^{-1} [17]. The absorption peak of the P-O group in PV appears at 950 cm^{-1} [18]. For CI and CIP$_{1.0}$, there is no absorption peak at 1690 cm^{-1}, confirming the reaction of the aldehyde group in PV and CV with the amino group in IPDA. Correspondingly, the Schiff base peak appears at 1650 cm^{-1} in the FTIR spectra of both CI and CIP$_{1.0}$ [19]. In addition, CIP$_{1.0}$ also shows a distinct absorption peak at 950 cm^{-1}. There are no obvious amino absorption peaks in the FTIR spectra of CI and CIP$_{1.0}$. All these indicate that CI and CIP$_{1.0}$ are successfully prepared by the reaction between -NH$_2$ and -CHO groups.

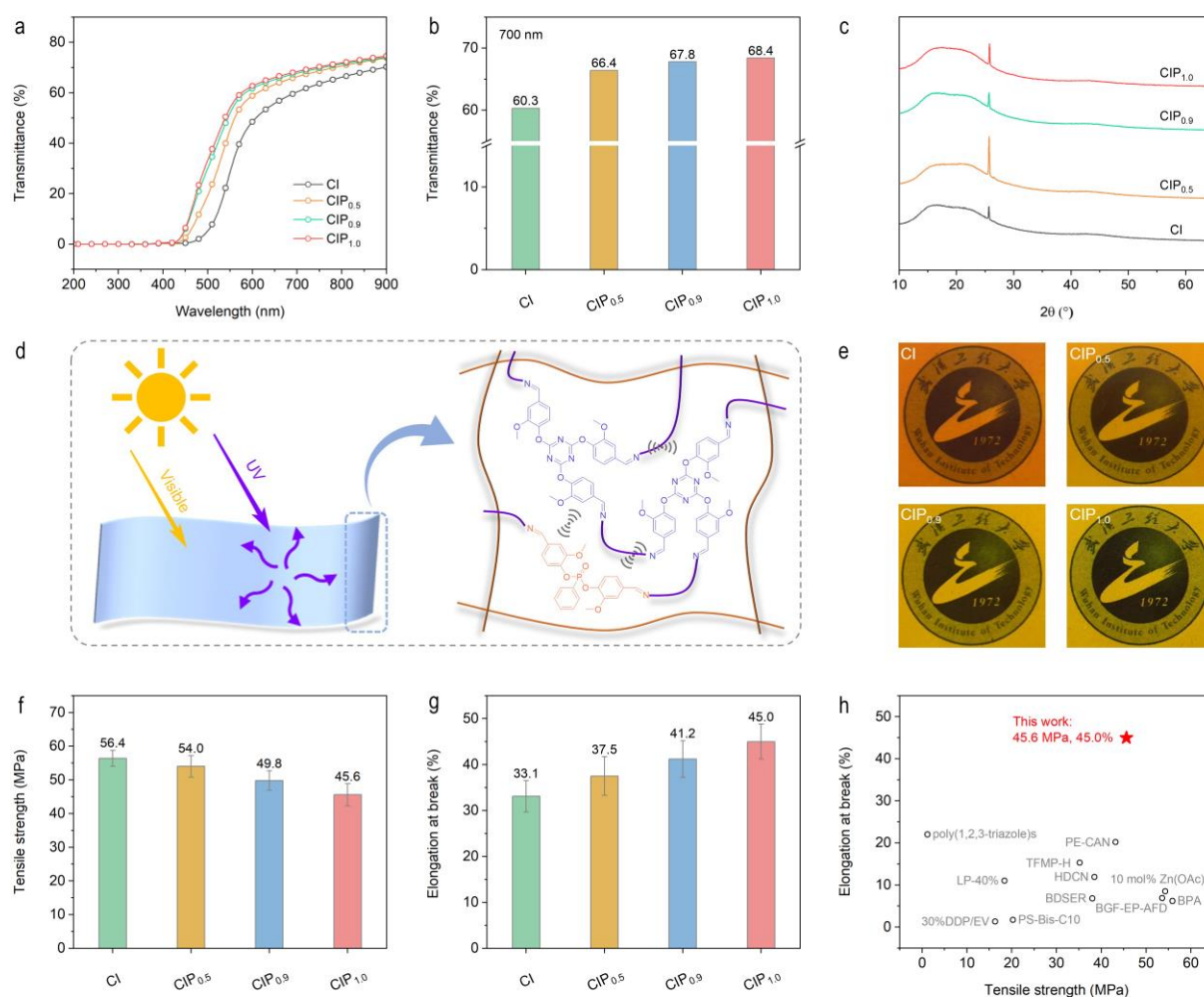### 3.2. Optical and mechanical properties

Fig. 2. (a) UV-visible transmission spectra and (c) XRD patterns of vitrimers; (b) the transmittance of vitrimers at 700 nm; (d) illustration of a possible mechanism for UV-resistance and π-π stacking; (e) digital images of vitrimer films; (f) tensile strength and (g) elongation at break of vitrimers; (h) comparison of elongation at break and tensile strength for $CIP_{1.0}$ and previously-reported vitrimers.

The high transparency of thermosetting resin makes it ubiquitous in optical devices, transportation, and other fields [20, 21]. Therefore, developing transparent vitrimers will greatly contribute to their industrialization. The UV-visible spectra of the vitrimer are shown in Fig. 2a. It is obvious that the transmittance of vitrimers in the range of 200-400 nm is approximately 0. It shows that all the resulting vitrimers have excellent UV-shielding functions. Immediately, the transmittance of all samples increases gradually with increasing

9

wavelength (400-900 nm). In addition, at the same wavelength, the transmittance of the vitrimer increases with increasing phosphorus content. Specifically, $CIP_{1.0}$ has the highest transmittance of 68.4% at 700 nm among all samples (see Fig. 2b). Thus, the transparency of $CIP_{1.0}$ is higher than that of CI (see Fig. 2e). The transparency of vitrimer is related to its crystalline properties [22, 23]. Therefore, the X-ray diffraction (XRD) technique is applied to investigate the crystalline properties of vitrimer, with the patterns shown in Fig. 2c. All vitrimers show a broad diffraction peak cantered around at $2\theta = 20°$ of all vitrimers. Thus, a well-cross-linked reaction occurs between CV, PV, and IPDA without significantly affecting the amorphous properties of the vitrimer, maintaining high transparency. Notably, all vitrimers have a sharp diffraction peak at $2\theta = 25.7°$ (d = 3.5 Å), which confirms that they are all partially crystallized with an ordered structure [24, 25]. The conjugated polymers with rigid structures exhibit strong π-π interchain interactions in the aggregated state [26, 27]. The d-spacing laminar is in the range of π-π stacking distance, which can be assigned to the π-π stacking of phenyl groups in the vitrimer network. The strong π-π stacking is also positively correlated with great UV shielding and toughness (see Fig. 2d).

The tensile properties of vitrimers were investigated in detail (see Fig. 2f-h). As shown in Fig. 2f-h, the tensile strength of the vitrimers gradually decreases with increasing PV content, while the elongation at break gradually increases, which may be related to the increase in the average molecular weight (M_c) of the chain between the two neighboring crosslinking points. Specifically, the tensile strength of all vitrimers is higher than 45 MPa and the elongation at break of all vitrimers is greater than 30.0%. In particular, the tensile strength and elongation at break of $CIP_{1.0}$ reach 45.6 MPa and 45.0%, respectively. The higher elongation at break and tensile strength of $CIP_{1.0}$ than previous vitrimers demonstrate its excellent mechanical strength and toughness (see Fig. 2h) [13, 28-37]. The high strength and toughness of $CIP_{1.0}$ are related to the π-π stacking effect between molecular chains and the appropriate

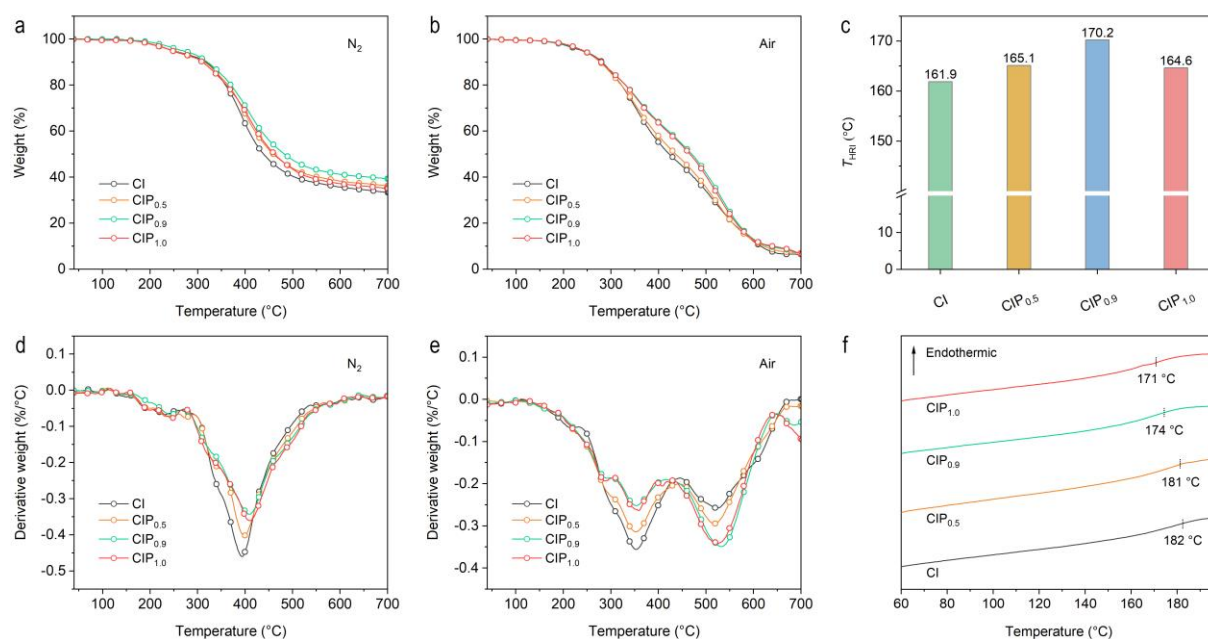crosslinking density.

3.3. Thermal performances

Fig. 3. (a) TG and (d) DTG curves of vitrimers in N_2 condition; (b) TG and (e) DTG curves of vitrimers under air flow; (c) T_{HRI} values and (f) DSC curves of vitrimers.

Thermogravimetric analysis (TGA) of vitrimers was conducted under nitrogen and air atmosphere, and the TG and derivative TG (DTG) curves are displayed in Fig. 3a-b and d-e. The characteristic thermal data, including temperature at 5% weight loss ($T_{5\%}$), temperature at maximum weight loss rate (T_{max}), maximum weight loss rate (R_{max}), and char yield at 700 °C (*CY*), are summarized in Table S2. The $T_{5\%}$ values of all vitrimers are basically the same in nitrogen and air atmosphere. For instance, the $T_{5\%}$ values of CI are 250 and 239 °C under nitrogen and air, and those of CIP$_{1.0}$ are 246 and 241 °C, respectively. Furthermore, the heat-resistance index (T_{HRI}) values of all vitrimers are determined based on previous works to further characterize their thermal stability [38, 39], with the results shown in Fig. 3c. Clearly, the T_{HRI} values of the CIP$_x$ samples are improved compared to that of CI. The results indicate that the addition of PV enhances the thermal stability of the vitrimer, making it superior to many typical phosphorus-based flame retardants because most of them deteriorate the

11

thermal stability by catalyzing degradation [40]. As illustrated in Table S2, the T_{max} value for CIP$_x$ samples are basically higher than that of CI and increase with increasing phosphorus content in both nitrogen and air conditions, further confirming the improved thermal stability. In addition, all vitrimers have high *CY* values under nitrogen and air atmosphere, suggesting that they have superior char-forming abilities at high temperatures, which may be related to the presence of Schiff base and phosphorus-containing groups. To summarize, the addition of PV maintains the thermal stability of CIP$_x$ effectively and enhances the char-forming ability dramatically.

The glass transition temperature (T_g) of the vitrimers was tested by differential scanning calorimetry (DSC), with the data shown in Fig. 3f. There is a decrease in the T_g from 182 °C for CI to 171 °C for CIP$_{1.0}$ with the introduction of PV, which may be related to the decrease in cross-linking density. However, the T_g of all vitrimers is higher than 170 °C, which is still adapted to most of the high-temperature application scenarios.

3.4. Flame-retardant performances and mechanisms
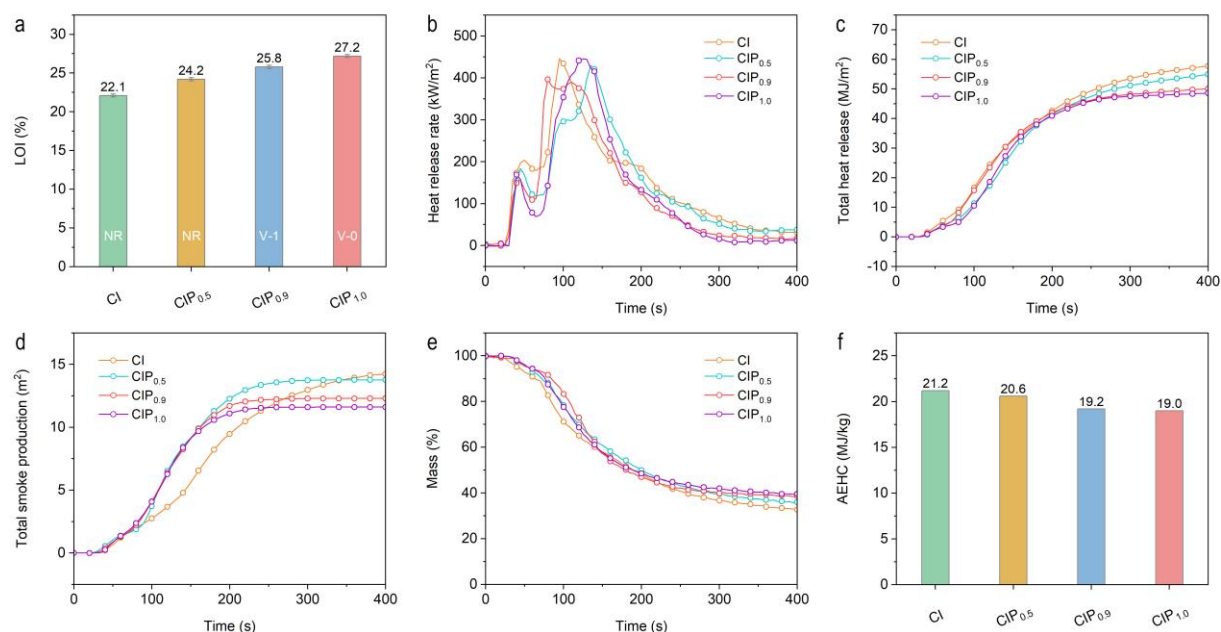

Fig. 4. (a) LOI and UL-94 results, (b) heat release rate curves, (c) total heat release plots, (d) total smoke production plots, (e) mass loss curves, and (f) AEHC values of vitrimers.

LOI and UL-94 tests were conducted on CI and CIP_x, with data presented in Fig. 4a. Despite exhibiting an LOI of 22.1%, the CI vitrimer cannot pass the UL-94 test, indicative of poor flame retardancy. Subsequently, PV is introduced into the cross-linked network to improve the flame retardancy of the vitrimer. Both LOI and UL-94 ratings are dramatically improved with the incorporation of PV. Specifically, the $CIP_{0.9}$ achieves an LOI of 25.8% and passes a UL-94 V-1 rating. The $CIP_{1.0}$ passes a UL-94 V-0 with a high LOI of 27.2% when the phosphorus content further increases to 1.0 wt%. The results indicate that the P element plays an important role in enhancing the fire retardancy of CIP_x vitrimers [41-43].

To investigate the combustion behaviors of CI and CIP_x, a cone calorimetry test (CCT) was performed, and the results are shown in Fig. 4b-f and S2. Significantly, CI and CIP_x exhibit a lower peak heat release rate (PHRR, ~ 450 kW/m^2). It is shown that the Schiff base provides an appropriate flame-retardant effect. Importantly, the total heat release (THR) and total smoke production (TSP) of CIP_x show a similar downtrend, demonstrating significantly improved flame retardancy and smoke suppression. For instance, compared with CI, the THR and TSP of $CIP_{1.0}$ are reduced by 20.6% and 19.4%, respectively (see Fig. 4b-d). At the same time, the char mass of $CIP_{1.0}$ reaches up to 39.5 wt%, which is about 20.8% higher than that of CI (see Fig. 4e). The PV facilitates the vitrimer matrix to form a protection residual layer during burning. Such a layer prevents the diffusion of heat and combustible gas and thus improves the flame retardancy of vitrimer. Smoke accounts for the dominant factor of casualties in fires, and the reduced TSP of CIP_x also shows that PV can inhibit the production of smoke, which can further improve the survival rate of personnel in fires. In addition, the average effective heat of combustion (AEHC) decreases with the introduction of PV (see Fig. 4f). It shows that the intensity of the combustion for gas-phase volatiles is decreased with the addition of PV [44, 45]. The radical-quenching effect of the P-containing decomposition fragments from PV is responsible for the reduced gas-phase combustion of the matrix.

Moreover, based on the photographs of residual chars after CCT (see Fig. S2), the residual char thickness of CI increases to 31 mm and the char layer is broken. In particular, the residual char of CIP$_{1.0}$ is continuous and dense with a thickness of 60 mm, which is 93.5% higher than that of CI. In conclusion, although the P-containing decomposition products of PV suppress the burning in the gas phase, they mainly function in the condensed phase to facilitate the char formation during burning, thus simultaneously enhancing flame retardancy and smoke suppression of vitrimers.
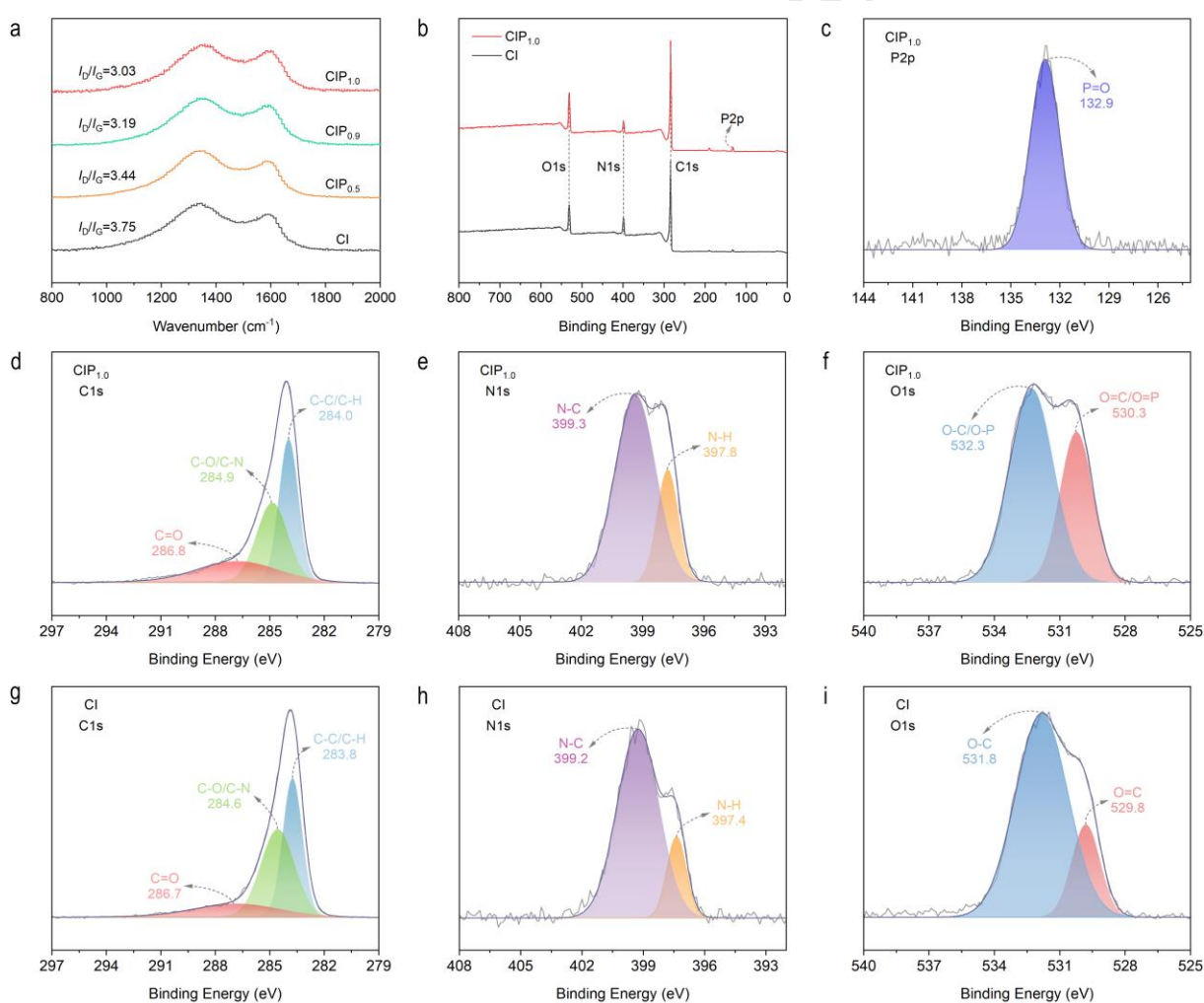

Fig. 5. (a) Raman spectra of residual chars for vitrimers; (b) XPS spectra of residual chars for CI and CIP$_{1.0}$; the high-resolution XPS (c) P2p, (d) C1s, (e) N1s, and (f) O1s spectra of residual char for CIP$_{1.0}$; and the high-resolution XPS (g) C1s, (h) N1s, and (i) O1s spectra of the residual char for CI.

14

To characterize the condensed-phase mode-of-action, Raman and X-ray photoelectron spectroscopy (XPS) tests were carried out to investigate the degree of graphitization, chemical composition, and bonding state of the vitrimer char from CCT. The residual chars display the D and G bands at 1360 and 1605 cm^{-1}, belonging to the amorphous carbon and graphite structures, respectively (see Fig. 5a). The integral area ratio of the D-band to the G-band (I_D/I_G) is directly related to the graphitization degree of char [46-48]. With increasing phosphorus content, the I_D/I_G value of residual char monotonically decreases, indicative of an increased degree of graphitization. Hence, the decomposition products of PV facilitate the charring of vitrimer and increase the degree of graphitization of the residual char during combustion, which inhibits heat release and oxygen transfer. In the C1s spectrum of CIP$_{1.0}$ char, three deconvolution peaks belonging to C=O, C-O/C-N, and C-C/C-H are detected. In the N1s spectrum, two peaks attributed to N-C and N-H appear, and in the O1s spectrum, two deconvolution peaks assigned to O-C/P and O=C/P are observed in CIP$_{1.0}$ char (see Fig. 5d-f) [49]. In addition to the above elements, the P (2.97 wt%) element can be detected in the char of CIP$_{1.0}$ (see Fig. 5b). In addition, P=O groups are identified in the P2p spectrum of CIP$_{1.0}$ char (see Fig. 5c), indicating that the condensed-phase decomposition products of PV are the phosphate derivatives. Meanwhile, the N content of CIP$_{1.0}$ char increases from 7.64 wt% of CI char to 11.47 wt% (see Table S3), which implies that the decomposition products of P-containing groups for PV have reacted with the N-containing groups in vitrimer during burning, leading to increased nitrogen content. In summary, the P-containing decomposition products of PV and Schiff base in vitrimer catalyze the matrix to form a compact and expanded char with a high graphitization degree on its surface during burning, which impedes the transfer of heat and protects the underlying substrate.

3.5. *Physical and chemical recovery*

Stress relaxation measurement is a commonly used method to study dynamic exchange reactions in vitrimer systems [3, 50, 51]. The stress relaxation curves of $CIP_{1.0}$ at different temperatures are shown in Fig. 6a. The relaxation time (τ^*) is the time required for the stress to decrease to 1/e of its initial value. As can be seen in Fig. 6a, the reaction rate of the imine exchange reaction within the $CIP_{1.0}$ network is relatively slow at 100 °C. The relaxation time decreases with increasing temperature, indicating that high temperature promotes the dynamic exchange reaction of the Schiff base. However, the overall relaxation time is short, which is related to the low cross-linking density of $CIP_{1.0}$. The activation energy (E_a) of the imine exchange reaction is calculated by fitting the τ^* value of $CIP_{1.0}$ to the Arrhenius equation: $\ln \tau^* = E_a/RT - \ln A$, where T is the absolute temperature, A is the pre-factor, and R is the gas constant [52]. The resulting linear fit curve shows an activation energy of 21.1 kJ/mol (see Fig. 6b). It indicates that the activation energy required for the dynamic exchange reaction within the $CIP_{1.0}$ network is relatively low and thus $CIP_{1.0}$ is easy to physically recover. We recovered the sheared $CIP_{1.0}$ film by hot pressing at 140 °C for 10 min, and the resulting film is noted as $CIP_{1.0}$-R. The tensile properties of $CIP_{1.0}$ and $CIP_{1.0}$-R are compared in Fig. 6c, and the tensile strength and elongation at break of $CIP_{1.0}$-R are 98.7% and 96.9% of those of $CIP_{1.0}$, respectively. Thus, it can be concluded that the Schiff base $CIP_{1.0}$ vitrimer can be applied sustainably.
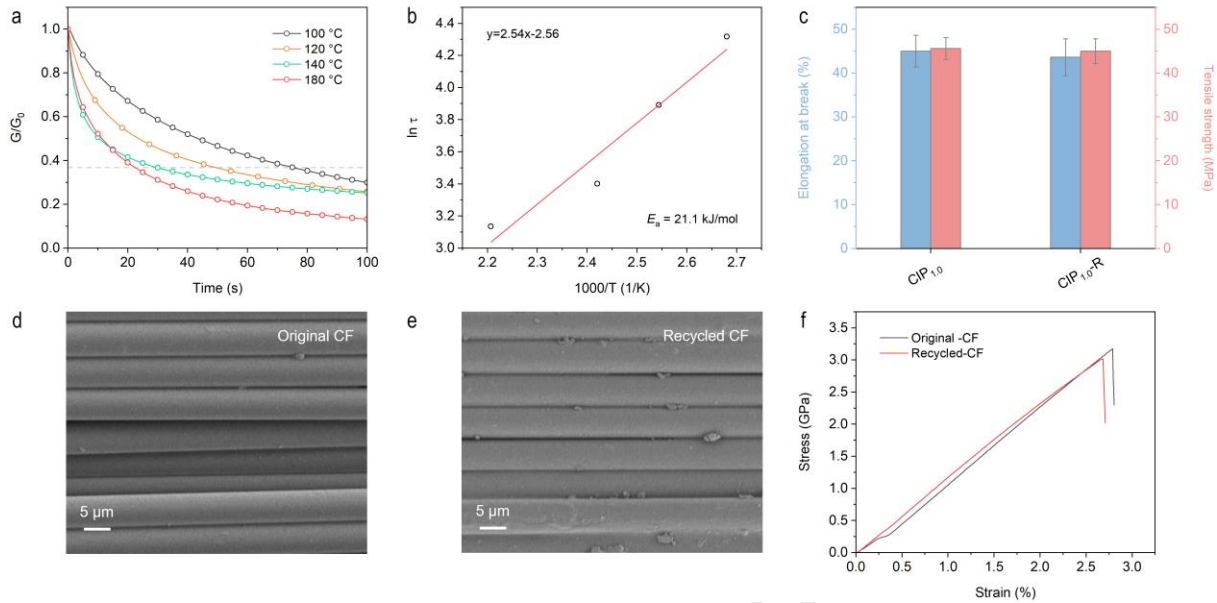
Fig. 6. (a) Normalized stress relaxation curves of $CIP_{1.0}$ at different temperatures; (b) linear fitting to the Arrhenius equation; (c) elongation at break and tensile strength of $CIP_{1.0}$ and $CIP_{1.0}$-Recycled ($CIP_{1.0}$-R); SEM of (d) original and (e) recycled CFs; (h) tensile stress-strain curves of original and recycled CFs.

The manufacture of carbon fiber-reinforced polymer composites is one major application for thermosetting resins. However, recycling CF is difficult with the composites based on thermoset resins. The dilemma can be solved with vitrimer. As the condensation and hydrolysis of imines are reversible reactions, the Schiff base vitrimer is usually considered to be a water- or acid-sensitive material [53]. Therefore, CFs can be recovered from CF/$CIP_{1.0}$ composites by chemical recycling. We immersed the fabricated CF/$CIP_{1.0}$ composites in THF/HCl (8 : 2) solution at 50 °C for 24 hours, and the $CIP_{1.0}$ was dissolved in the solution. The recovered CFs were washed with DMF and dried in an oven. The surface morphology and single fiber tensile properties of the recovered CFs were investigated, with the results shown in Fig. 6d-f. The recovered CFs exhibit a clean surface morphology, which is close to the original CFs, indicating that the $CIP_{1.0}$ is completely separated from the CFs. In addition, the tensile strength and elongation at break of the recycled CFs are 3.0 GPa and 2.6%, which are close to 3.2 GPa and 2.8% of the original CFs. Therefore, the well-designed $CIP_{1.0}$

vitrimer shows great promise for application in the preparation of advanced recyclable carbon fiber-reinforced polymer composites.

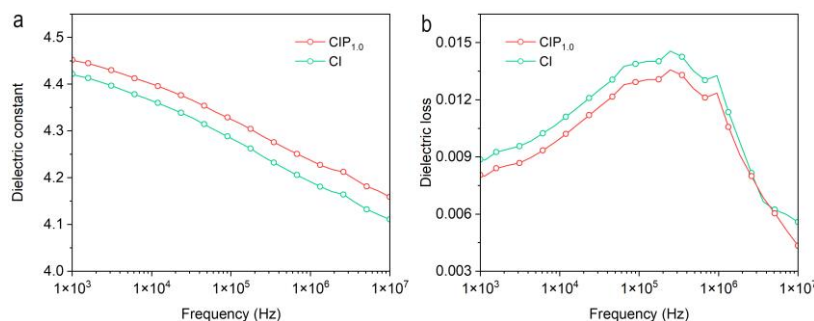### 3.6. Dielectric and antimicrobial properties

Fig. 7. (a) Dielectric constant and (b) dielectric loss of CI and CIP$_{1.0}$.

The low dielectric constant and loss are key to thermosetting resins for high-tech electrical and electronic applications [54]. Accordingly, the dielectric properties of CI and CIP$_{1.0}$ were investigated, and their dielectric constant and loss curves are shown in Fig. 7. There is a relatively stable dielectric constant and loss in the frequency range of $10^3 \sim 10^7$ Hz for CI and CIP$_{1.0}$. The dielectric constant and loss of CI and CIP$_{1.0}$ are very close. For instance, the dielectric constant of CI and CIP$_{1.0}$ is in the range of 4.1 to 4.5 and the dielectric loss of CI and CIP$_{1.0}$ is less than 0.015. Significantly, the dielectric properties of CI and CIP$_{1.0}$ are superior to those of thermosetting counterparts (dielectric constant = 4.7, dielectric loss = 0.018, at 10^3 Hz) [54]. It is associated with an abundance of highly symmetric, low-polar triazine groups in the CI and CIP$_{1.0}$ networks. Therefore, the CI and CIP$_{1.0}$ samples with low dielectric constant and loss are promising for a wide range of applications in electrical/electronic fields.
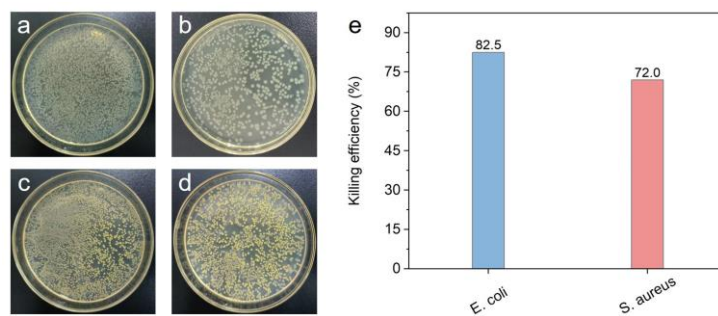
Fig. 8. Antibacterial photos of the blank group for (a) *E*. coil and (c) *S*. aureus; antibacterial photos of CIP$_{1.0}$ for (b) *E*. coil and (d) *S*. aureus; and (e) the antimicrobial rate of CIP$_{1.0}$ against *E*. coli and *S*. aureus.

Based on the presence of hydroxyl groups, lots of thermosets are usually hydrophilic and prone to harbor bacteria. In contrast, the Schiff base has potential antimicrobial activity, which is promising for its application in the antimicrobial industry. The standing *E*. coli and *S*. aureus are selected for antimicrobial evaluation. As shown in Fig. 8a-e, after 24 hours of incubation, the number of colonies in CIP$_{1.0}$ is significantly reduced, and its bactericidal rate against *E*. coli and *S*. aureus is 82.5% and 72.0%, respectively, with high antimicrobial performances (see Fig. 8e). The superior antimicrobial capacity of CIP$_{1.0}$ is attributed to its abundant Schiff base groups.

4. Conclusions

A biomass Schiff base vitrimer (CIP$_{1.0}$) was successfully synthesized using vanillin, cyanuric chloride and phenylphosphonic dichloride. As a result of the efficient structural design, the Schiff base groups are distributed uniformly within the vitrimer network, endowing the vitrimer with excellent comprehensive properties. The appropriate crosslinking density and intermolecular π-π stacking imbue the vitrimer with high toughness and dielectric properties. Meanwhile, CIP$_{1.0}$ also exhibits excellent condensed phase flame retardancy due to the high C=N and phosphate ester contents. CIP$_{1.0}$ can be applied to the carbon fiber-reinforced polymer composites as a polymer matrix, and the carbon fibers can be fully

recycled due to the degradability of $CIP_{1.0}$. The study has resulted in high-performance, multifunctional vitrimers derived from availably economical ingredients that have the potential to replace traditional thermosets in industrial sections, such as electronics, packaging, medical devices, and transportation.

Declaration of competing interest

The authors declare that they have no known competing financial interests or personal relationships that could have appeared to influence the work reported in this paper.

Acknowledgments

References

[1] Y. Jiang, J. Li, D. Li, Y. Ma, S. Zhou, Y. Wang, D. Zhang, Bio-based hyperbranched epoxy resins: synthesis and recycling, Chem. Soc. Rev. 53(2) (2024) 624-655. https://doi.org/10.1039/d3cs00713h.

[2] Z. Sun, Y. Luo, C. Chen, Z. Dong, G. Jiang, F. Chen, P. Ma, Mechanical enhancement of carbon fiber-reinforced polymers: From interfacial regulating strategies to advanced processing technologies, Prog. Mater. Sci. 142 (2024) 101221. https://doi.org/10.1016/j.pmatsci.2023.101221.

[3] Z. Hu, F. Hu, L. Deng, Y. Yang, Q. Xie, Z. Gao, C. Pan, Y. Jin, J. Tang, G. Yu, W. Zhang, Reprocessible Triketoenamine-Based Vitrimers with Closed-Loop Recyclability, Angew. Chem. Int. Edit. 62(34) (2023) e202306039. https://doi.org/10.1002/anie.202306039.

[4] P. Zamani, O. Zabihi, M. Ahmadi, R. Mahmoodi, T. Kannangara, P. Joseph, M. Naebe, Biobased Carbon Fiber Composites with Enhanced Flame Retardancy: A Cradle-to-Cradle

Approach, ACS Sustain. Chem. Eng. 10(2) (2021) 1059-1069. https://doi.org/10.1021/acssuschemeng.1c07859.

[5] M. Chen, W. Luo, S. Lin, B. Zheng, H. Zhang, Recyclable, reprocessable, self-healing elastomer-like epoxy vitrimer with low dielectric permittivity and its closed-loop recyclable carbon fiber reinforced composite, Compos. Part B: Eng. 257 (2023) 110666. https://doi.org/10.1016/j.compositesb.2023.110666.

[6] H. Si, L. Zhou, Y. Wu, L. Song, M. Kang, X. Zhao, M. Chen, Rapidly reprocessable, degradable epoxy vitrimer and recyclable carbon fiber reinforced thermoset composites relied on high contents of exchangeable aromatic disulfide crosslinks, Compos. Part B: Eng. 199 (2020) 108278. https://doi.org/10.1016/j.compositesb.2020.108278.

[7] J.-H. Chen, B.-W. Liu, J.-H. Lu, P. Lu, Y.-L. Tang, L. Chen, Y.-Z. Wang, Catalyst-free dynamic transesterification towards a high-performance and fire-safe epoxy vitrimer and its carbon fiber composite, Green Chem. 24(18) (2022) 6980-6988. https://doi.org/10.1039/d2gc01405j.

[8] W. Li, L. Xiao, J. Huang, Y. Wang, X. Nie, J. Chen, Bio-based epoxy vitrimer for recyclable and carbon fiber reinforced materials: Synthesis and structure-property relationship, Compos. Sci. Technol. 227 (2022) 109575. https://doi.org/10.1016/j.compscitech.2022.109575.

[9] W. He, P. Song, B. Yu, Z. Fang, H. Wang, Flame retardant polymeric nanocomposites through the combination of nanomaterials and conventional flame retardants, Prog. Mater. Sci. 114 (2020) 100687. https://doi.org/10.1016/j.pmatsci.2020.100687.

[10] Z. Miao, C. Peng, L. Xia, H. Xu, S. He, C. Chi, J. Zhong, S. Wang, W. Luo, G. Chen, B. Zeng, L. Dai, Fire-Safe Fully Bio-Based Schiff Base Epoxy Thermosets with Excellent Mechanical Properties and Adjustable Degradability, ACS Appl. Polym Mater. 5(8) (2023) 6325-6337. https://doi.org/10.1021/acsapm.3c00953.

[11] H. Nabipour, X. Wang, Y. Hu, Carbon fiber-reinforced composites based on an epoxy resin containing Schiff base with intrinsic anti-flammability, good mechanical strength and recyclability, Eur. Polym. J. 194 (2023) 112166. https://doi.org/10.1016/j.eurpolymj.2023.112166.

[12] H. Nabipour, H. Niu, X. Wang, S. Batool, Y. Hu, Fully bio-based epoxy resin derived from vanillin with flame retardancy and degradability, React. Funct. Polym. 168 (2021) 105034. https://doi.org/10.1016/j.reactfunctpolym.2021.105034.

[13] S. Wang, S. Ma, Q. Li, W. Yuan, B. Wang, J. Zhu, Robust, Fire-Safe, Monomer-Recovery, Highly Malleable Thermosets from Renewable Bioresources, Macromolecules 51(20) (2018) 8001-8012. https://doi.org/10.1021/acs.macromol.8b01601.

[14] J. Peng, S. Xie, T. Liu, D. Wang, R. Ou, C. Guo, Q. Wang, Z. Liu, High-performance epoxy vitrimer with superior self-healing, shape-memory, flame retardancy, and antibacterial properties based on multifunctional curing agent, Compos. Part B: Eng. 242 (2022) 110109. https://doi.org/10.1016/j.compositesb.2022.110109.

[15] J. Wan, J. Zhao, B. Gan, C. Li, J. Molina-Aldareguia, Y. Zhao, Y.-T. Pan, D.-Y. Wang, Ultrastiff Biobased Epoxy Resin with High T_g and Low Permittivity: From Synthesis to Properties, ACS Sustain. Chem. Eng. 4(5) (2016) 2869-2880. https://doi.org/10.1021/acssuschemeng.6b00479.

[16] X. Zhang, Q. Chi, C. Tang, H. Li, C. Zhang, Z. Li, T. Zhang, Achieving high-temperature resistance and excellent insulation property of epoxy by introducing triazine ring structure, J. Mater. Sci: Mater. 34(7) (2023) 638. https://doi.org/10.1007/s10854-023-10078-6.

[17] L. Jiang, Y. Tian, J. Cheng, J. Zhang, A biomass-based Schiff base vitrimer with both excellent performance and multiple degradability, Polym. Chem. 12(45) (2021) 6527-6537. https://doi.org/10.1039/d1py01003d.

[18] G. Ye, S. Huo, C. Wang, Q. Shi, L. Yu, Z. Liu, Z. Fang, H. Wang, A novel hyperbranched phosphorus-boron polymer for transparent, flame-retardant, smoke-suppressive, robust yet tough epoxy resins, Compos. Part B: Eng. 227 (2021) 109395. https://doi.org/10.1016/j.compositesb.2021.109395.

[19] M. Liu, F. Gao, X. Guo, Q. Liang, J. He, J. Zhong, C. Lin, F. Lin, L. Shen, Room temperature-curable, easily degradable, and highly malleable and recyclable vanillin-based vitrimers with catalyst-free bond exchange, Polym. Test. 115 (2022) 107740. https://doi.org/10.1016/j.polymertesting.2022.107740.

[20] Z. Xu, M. Wu, W. Gao, H. Bai, A Transparent, Skin-Inspired Composite Film with Outstanding Tear Resistance Based on Flat Silk Cocoon, Adv. Mater. 32(34) (2020) 2002695. https://doi.org/10.1002/adma.202002695.

[21] L.N. Saw, M. Mariatti, A.R. Azura, A. Azizan, J.K. Kim, Transparent, electrically conductive, and flexible films made from multiwalled carbon nanotube/epoxy composites, Compos. Part B: Eng. 43(8) (2012) 2973-2979. https://doi.org/10.1016/j.compositesb.2012.05.048.

[22] C. Wang, S. Huo, G. Ye, P. Song, H. Wang, Z. Liu, A P/Si-containing polyethylenimine curing agent towards transparent, durable fire-safe, mechanically-robust and tough epoxy resins, Chem. Eng. J. 451 (2023) 138768. https://doi.org/10.1016/j.cej.2022.138768.

[23] G. Ye, S. Huo, C. Wang, Q. Zhang, B. Wang, Z. Guo, H. Wang, Z. Liu, Fabrication of flame-retardant, strong, and tough epoxy resins by solvent-free polymerization with bioderived, reactive flame retardant, Sustain. Mater. Techno. 39 (2024) e00853. https://doi.org/10.1016/j.susmat.2024.e00853.

[24] S. Zhang, B. Yang, D. Liu, H. Zhang, W. Zhao, Q. Wang, C. He, J. Hou, Correlations among Chemical Structure, Backbone Conformation, and Morphology in Two Highly

Efficient Photovoltaic Polymer Materials, Macromolecules 49(1) (2015) 120-126. https://doi.org/10.1021/acs.macromol.5b02416.

[25] M. Ma, N. Dai, X. Liu, C. Li, Q. Yuan, F. Huang, Reinforcing the poly(silylene arylacetylene)s via strong π-π stacking interactions, Polymer 229 (2021) 123976. https://doi.org/10.1016/j.polymer.2021.123976.

[26] Y.-P. Ni, Q.-T. Li, L. Chen, W.-S. Wu, Z.-H. Qin, Y. Zhang, L. Chen, X.-L. Wang, Y.-Z. Wang, Semi-aromatic copolyesters with high strength and fire safety via hydrogen bonds and π-π stacking, Chem. Eng. J. 374 (2019) 694-705. https://doi.org/10.1016/j.cej.2019.05.212.

[27] L. Chen, H.-B. Zhao, Y.-P. Ni, T. Fu, W.-S. Wu, X.-L. Wang, Y.-Z. Wang, 3D printable robust shape memory PET copolyesters with fire safety via π-stacking and synergistic crosslinking, J. Mater. Chem. A 7(28) (2019) 17037-17045. https://doi.org/10.1039/c9ta04187g.

[28] X. Feng, G. Li, Versatile Phosphate Diester-Based Flame Retardant Vitrimers via Catalyst-Free Mixed Transesterification, ACS Appl. Mater. Inter. 12(51) (2020) 57486-57496. https://doi.org/10.1021/acsami.0c18852.

[29] Y. Zhang, H. Yan, R. Yu, J. Yuan, K. Yang, R. Liu, Y. He, W. Feng, W. Tian, Hyperbranched Dynamic Crosslinking Networks Enable Degradable, Reconfigurable, and Multifunctional Epoxy Vitrimer, Adv. Sci. 11(2) (2024) e2306350. https://doi.org/10.1002/advs.202306350.

[30] X. Feng, G. Li, Catalyst-free β-hydroxy phosphate ester exchange for robust fire-proof vitrimers, Chem. Eng. J. 417 (2021) 129132. https://doi.org/10.1016/j.cej.2021.129132.

[31] J.H. Chen, J.H. Lu, X.L. Pu, L. Chen, Y.Z. Wang, Recyclable, malleable and intrinsically flame-retardant epoxy resin with catalytic transesterification, Chemosphere 294 (2022) 133778. https://doi.org/10.1016/j.chemosphere.2022.133778.

[32] F. Zhou, Z. Guo, W. Wang, X. Lei, B. Zhang, H. Zhang, Q. Zhang, Preparation of self-healing, recyclable epoxy resins and low-electrical resistance composites based on double-disulfide bond exchange, Compos. Sci. Technol. 167 (2018) 79-85. https://doi.org/10.1016/j.compscitech.2018.07.041.

[33] Y. Nishimura, J. Chung, H. Muradyan, Z. Guan, Silyl Ether as a Robust and Thermally Stable Dynamic Covalent Motif for Malleable Polymer Design, J. Am. Chem. Soc. 139(42) (2017) 14881-14884. https://doi.org/10.1021/jacs.7b08826.

[34] M.M. Obadia, B.P. Mudraboyina, A. Serghei, D. Montarnal, E. Drockenmuller, Reprocessing and Recycling of Highly Cross-Linked Ion-Conducting Networks through Transalkylation Exchanges of C-N Bonds, J. Am. Chem. Soc. 137(18) (2015) 6078-6083. https://doi.org/10.1021/jacs.5b02653.

[35] J. Liu, K.V. Bernaerts, Preparation of lignin-based imine vitrimers and their potential application as repairable, self-cleaning, removable and degradable coatings, J. Mater. Chem. A 12(5) (2024) 2959-2973. https://doi.org/10.1039/d3ta06338k.

[36] S. Tang, H. Lin, K. Dong, J. Zhang, C. Zhao, Closed-loop recycling and degradation of guaiacol-based epoxy resin and its carbon fiber reinforced composites with S-S exchangeable bonds, Polym. Degrad. Stabil. 210 (2023) 110298. https://doi.org/10.1016/j.polymdegradstab.2023.110298.

[37] D. Montarnal, M. Capelot, F. Tournilhac, L. Leibler, Silica-Like Malleable Materials from Permanent Organic Networks, Science 334 (2011) 965-968. https://doi.org/10.1126/science.1212648.

[38] J. Gu, Z. Lv, Y. Wu, Y. Guo, L. Tian, H. Qiu, W. Li, Q. Zhang, Dielectric thermally conductive boron nitride/polyimide composites with outstanding thermal stabilities via in-situ polymerization-electrospinning-hot press method, Compos. Part A: Appl. S. 94 (2017) 209-216. https://doi.org/10.1016/j.compositesa.2016.12.014.

[39] Z. Liu, J. Zhang, L. Tang, Y. Zhou, Y. Lin, R. Wang, J. Kong, Y. Tang, J. Gu, Improved wave-transparent performances and enhanced mechanical properties for fluoride-containing PBO precursor modified cyanate ester resins and their PBO fibers/cyanate ester composites, Compos. Part B: Eng. 178 (2019) 107466. https://doi.org/10.1016/j.compositesb.2019.107466.

[40] J. Zhang, X. Mi, S. Chen, Z. Xu, D. Zhang, M. Miao, J. Wang, A bio-based hyperbranched flame retardant for epoxy resins, Chem. Eng. J. 381 (2020) 122719. https://doi.org/10.1016/j.cej.2019.122719.

[41] B.W. Liu, H.B. Zhao, Y.Z. Wang, Advanced Flame-Retardant Methods for Polymeric Materials, Adv. Mater. 34(46) (2022) 2107905. https://doi.org/10.1002/adma.202107905.

[42] J. Zeng, F. Lin, W. Hsu, S. Wang, Y. Wu, X. Wang, H. Cheng, Q. Zhu, H. Wu, L. Song, Synthesis of cerium-based flame retardant containing phosphorus and its impact on the flammability of polylactic acid, Int. J. Biol. Macromol. 271 (2024) 132636. https://doi.org/10.1016/j.ijbiomac.2024.132636.

[43] M.-H. Zhou, X. Ao, M. Islam, Y.-Y. Liu, S.G. Prolongo, D.-Y. Wang, Bio-based epoxy vitrimer with inherent excellent flame retardance and recyclability via molecular design, Int. J. Biol. Macromol. 262 (2024) 129363. https://doi.org/10.1016/j.ijbiomac.2024.129363.

[44] J. Feng, Y. Lu, H. Xie, Z. Xu, G. Huang, C.-F. Cao, Y. Zhang, V.S. Chevali, P. Song, H. Wang, Solvent-Free Synthesis of Organic-Inorganic Polyphosphoramide-Halloysite Nanohybrids for Thermally Stable and Fire-Resistant Polylactide, ACS Sustain. Chem. Eng. 10(46) (2022) 15223-15232. https://doi.org/10.1021/acssuschemeng.2c04899.

[45] M. Tao, L. Qian, J. Wang, H. Zhu, W. Tang, Y. Chen, W. Xi, Y. Qiu, From physical mixtures to block copolymer: Impose outstandingly toughening and flame retardant effect to polypropylene, Compos. Part B: Eng. 253 (2023) 110538. https://doi.org/10.1016/j.compositesb.2023.110538.

[46] L. Yu, S. Huo, C. Wang, G. Ye, P. Song, J. Feng, Z. Fang, H. Wang, Z. Liu, Flame-retardant poly(L-lactic acid) with enhanced UV protection and well-preserved mechanical properties by a furan-containing polyphosphoramide, Int. J. Biol. Macromol. 234 (2023) 123707. https://doi.org/10.1016/j.ijbiomac.2023.123707.

[47] Z. Zhang, S. Huo, L. Yu, G. Ye, C. Wang, Q. Zhang, Z. Liu, A generalizable reactive blending strategy to construct flame-retardant, mechanically-strong and toughened poly(L-lactic acid) bioplastics, Int. J. Biol. Macromol. 265 (2024) 130806. https://doi.org/10.1016/j.ijbiomac.2024.130806.

[48] G. Yang, W.H. Wu, Y.H. Wang, Y.H. Jiao, L.Y. Lu, H.Q. Qu, X.Y. Qin, Synthesis of a novel phosphazene-based flame retardant with active amine groups and its application in reducing the fire hazard of Epoxy Resin, J. Hazard. Mater. 366 (2019) 78-87. https://doi.org/10.1016/j.jhazmat.2018.11.093.

[49] F. Wei, J. Zhang, C. Wu, M. Luo, B. Ye, H. Zhang, J. Wang, M. Miao, T. Li, D. Zhang, Closed-Loop Recycling of Tough and Flame-Retardant Epoxy Resins, Macromolecules 56(14) (2023) 5290-5305. https://doi.org/10.1021/acs.macromol.3c00650.

[50] C. Tretbar, J. Castro, K. Yokoyama, Z. Guan, Fluoride-Catalyzed Siloxane Exchange as a Robust Dynamic Chemistry for High-Performance Vitrimers, Adv. Mater. 35(28) (2023) 2303280. https://doi.org/10.1002/adma.202303280.

[51] Y. Yang, S. Zhang, X. Zhang, L. Gao, Y. Wei, Y. Ji, Detecting topology freezing transition temperature of vitrimers by AIE luminogens, Nat. Commun. 10 (2019) 3165. https://doi.org/10.1038/s41467-019-11144-6.

[52] Y. Liu, Z. Yu, G. Lu, W. Chen, Z. Ye, Y. He, Z. Tang, J. Zhu, Versatile levulinic acid-derived dynamic covalent thermosets enabled by in situ generated imine and multiple hydrogen bonds, Chem. Eng. J. 451 (2023) 139053. https://doi.org/10.1016/j.cej.2022.139053.

[53] T. Liu, J. Peng, J. Liu, X. Hao, C. Guo, R. Ou, Z. Liu, Q. Wang, Fully recyclable, flame-retardant and high-performance carbon fiber composites based on vanillin-terminated cyclophosphazene polyimine thermosets, Compos. Part B: Eng. 224 (2021) 109188. https://doi.org/10.1016/j.compositesb.2021.109188.

[54] S. Huo, T. Sai, S. Ran, Z. Guo, Z. Fang, P. Song, H. Wang, A hyperbranched P/N/B-containing oligomer as multifunctional flame retardant for epoxy resins, Compos. Part B: Eng. 234 (2022) 109701. https://doi.org/10.1016/j.compositesb.2022.109701.